AN X-RAY DOUBLE CRYSTAL SPECTROMETER STUDY OF Ar and Rb IMPLANTED MgO CRYSTALS

by

BASIL LEE SNEERINGER

B.A., Kansas State College of Pittsburg, 1974

A MASTER'S THESIS

submitted in partial fulfillment of the

requirements for the degree

MASTER OF SCIENCE

Department of Physics

KANSAS STATE UNIVERSITY
Manhattan, Kansas

1976

R. Dean Gragsdorf
Major Professor

TABLE OF CONTENTS

LIST OF FIGURES

LIST OF PLATES

LIST OF TABLES

INTRODUCTION

Many of the physical properties of solids depend to a large extent on the perfection of the crystals from which solids are built. Hence the problem of defects in crystals is of interest to those who are searching for new methods to improve the mechanical and electrical properties of materials. The double crystal spectrometer can be useful in providing information about the perfection of crystals.

This paper is a study of the average effect of lattice damage in MgO due to the implantation of ions of Rubidium and Argon. This study was implemented by the comparison of rocking curves of unimplanted and Rubidium and Argon implanted MgO taken with a double crystal spectrometer set in the parallel position. In this paper we will limit ourselves to the study of the full width of the rocking curve at half maximum and attempt to indicate that on the average the crystal lattice is strained in a manner which preserves the symmetry of the rocking curve while increasing the full width at half maximum.

Although the use of the double crystal spectrometer is well established, it is not so widely applied to the study of lattice damage. A search of the literature indicates that the double crystal spectrometer was used by Workman and Dragsdorf[1] in a study of the implantation of singly-ionized sodium ions in MgO. Other studies cited by Workman taking

advantage of the high precision and absence of dispersion in the parallel (1,-1) position of the double crystal spectrometer include papers by Thomas, Baldwin and Dederichs[2]; Kishino and Noda[3]; Petry and Pluchery[4]; Patel, Wagner and Moss[5]; and Bachman, Baldwin and Young[6].

Theoretical work with respect to the interpretation of the rocking curves was first given by Darwin[7], Ewald[8], and von Laue[9]. Introductory treatment is given in books by James[10], Zachariasen[11], Compton and Allison[12], and Warren[13]. Advanced treatment of the dynamical theory may be found in Azaroff et al.[14] along with a number of excellent references. Advanced treatment of the interpretation of the rocking curves is given by Krivoglaz[15].

THEORY

A brief sketch of the theory involved in utilizing the double crystal spectrometer to study lattice damage is presented. The Bragg reflection from a set of crystal planes taking into account multiple reflections is first discussed. The implications this treatment has for the double crystal spectrometer in terms of the convolution of the reflected intensity from the monochromating and analyzing crystals, i.e. the rocking curve, is then observed. The treatment given here will follow closely that of Darwin[7] for simplicity of introduction. The details may be found in Warren[13] and James[10].

The intensity of reflection from a regular array of N atoms per unit volume which form a set of parallel lattice planes spaced a distance d apart will be considered. It is assumed that the incident radiation is highly monochromatic and parallel to within a few seconds of arc. The planes are indexed by the letter r in a manner such that r = 0 will denote the surface plane as shown in Fig. 1. T_r and S_r represent the incident and reflected amplitudes respectively just above the rth plane.

The object of the calculation is to obtain the ratio of the reflected to incident reflection coefficients at the surface of the crystal. This ratio, S_o/T_o, can be squared to yield the ratio of reflected to incident intensities I/I_o.

Figure 1. Indexing of crystal planes.

THIS BOOK CONTAINS NUMEROUS PAGES WITH DIAGRAMS THAT ARE CROOKED COMPARED TO THE REST OF THE INFORMATION ON THE PAGE.

THIS IS AS RECEIVED FROM CUSTOMER.

FIGURE 1

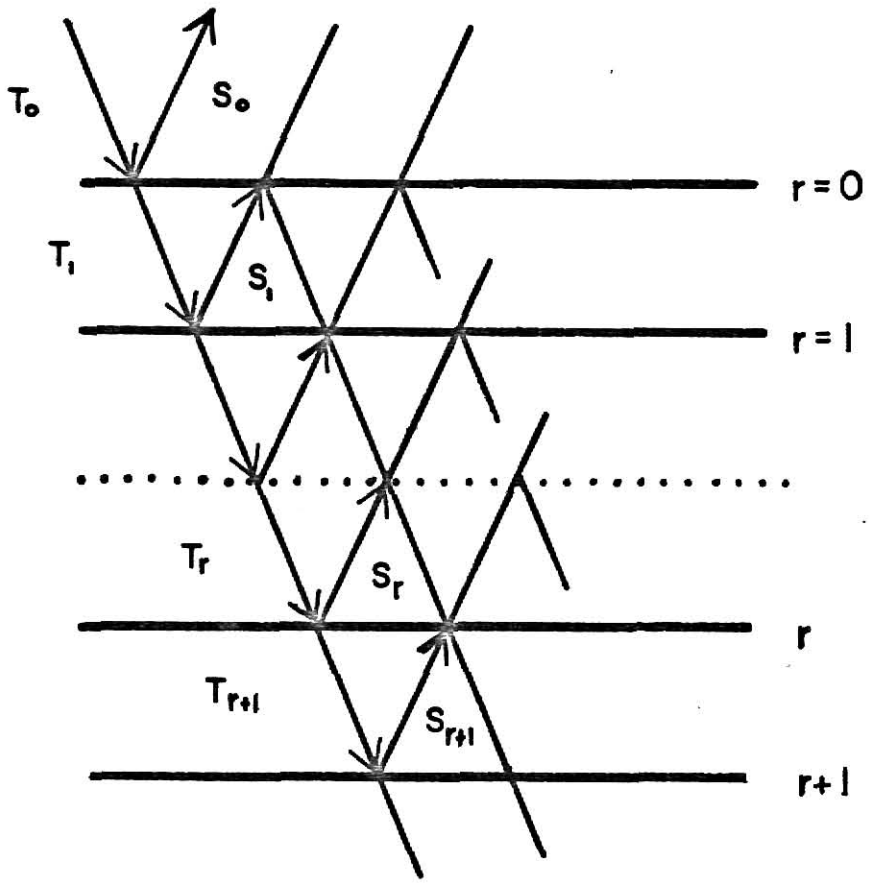

The idea behind this calculation involves the interchange of energy between the incident and reflected beams. S_r must consist of that part of T_r which is transmitted through the rth plane from below. Likewise, T_{r+1} must consist of that part of T_r which is transmitted through the rth plane from above plus that part of S_r which is reflected from the lower side of the rth plane.

The complex reflection coefficient which takes into account the $\pi/2$ phase shift upon reflection as well as the amplitude of the reflected wave is according to a formula first given by Darwin,

$$iq = i(Nd\lambda/\sin\theta)\, F(2\theta)\, (e^2/mc^2) \qquad (1)$$

where i is the imaginary number $i = (-1)^{\frac{1}{2}}$, N is the number of atoms per unit volume, d is the distance between lattice planes, e is the electronic charge of an electron, m is the mass of an electron, c is the speed of light, θ is the Bragg angle, λ is the wavelength of the incident radiation and $F(2\theta)$ is the structure factor of a unit group of atoms for radiation scattered through an angle 2θ. The transmission coefficient is given by

$$-iq_o = i(Nd\lambda/\sin\theta)\, F(0)\, (e^2/mc^2) \qquad (2)$$

where F(0) is the structure factor of a unit group of atoms for a forward scattered wave.

The amplitude of the reflected beam is just the difference between the incident amplitude A and the transmitted amplitude $(-iq_o)A$ which is just $(1 + iq_o)A$ for no absorption. If absorption is included, where h is the absorption coefficient and h is small, then the transmitted amplitude is given by the product $(1 + iq_o)(1 - h)A$. Negelecting higher order terms the amplitude may be written $(1 - h + iq_o)A$.

The reflection from the rth plane, S_r, with absorption becomes

$$S_r = T_r iq + (1 - h + iq_o)S_{r+1}e^{-i\phi} \qquad (3)$$

where the fraction of S_{r+1} transmitted through the rth plane must be taken at the rth plane, so this is $(1 + iq_o - h)S_{r+1}e^{-i\phi}$ instead of merely S_{r+1}. The phase difference corresonding to the path difference 'd sin θ' is

$$\phi = (2\pi/\lambda)d \sin \theta \ . \qquad (3a)$$

With the phase consideration in mind we see that this leads to

$$T_{r+1} = (1 - h + iq_o)T_r e^{-i\phi} + iqS_{r+1}e^{-2i\phi} \qquad (4)$$

where the phase factor $e^{-i\phi}$ comes in twice in the second term above.

This is the second of the two difference equations that Darwin used to arrive at the coefficient ratio

$$S_o/T_o = iq/(h + iv \pm (q^2 + (h + iv)^2)^{\frac{1}{2}}) \qquad (5)$$

where v is a small difference in phase due to a deviation in Braggs law stemming from the slight change of phase q_o in passing through a sheet of atoms. The difference v is

$$v = (2\pi d/\lambda)\cos\theta(\theta - \theta_o) \qquad (6)$$

where θ_o is the Bragg angle corrected for the index of refraction.

Reparameterizing equation 6 in terms of more familiar angular variables, the ratio S_o/T_o is given by

$$S_o/T_o = is/(b + ie \pm (s^2 + (b + ie)^2)^{\frac{1}{2}}) \qquad (7)$$

where we have introduced the three parameters

$$e = \theta - \theta_o = v\lambda/2\pi d\cos\theta \qquad (8)$$
$$s = q\lambda/2\pi d\cos\theta$$
$$b = h\lambda/2\pi d\cos\theta$$

If absorption is small with respect to the reflected intensity, we may set b = 0 and obtain

$$S_o/T_o = is/(ie \pm (s^2 - e^2)^{\frac{1}{2}}) \ . \qquad (9)$$

Upon squaring the above expression, I/I_o is obtained for three regions. Thus

$$\begin{aligned} e < -s \qquad & I/I_o = s^2/(e - (e^2 - s^2)^{\frac{1}{2}})^2 \\ -s < e < s \qquad & I/I_o = 1 \\ e > s \qquad & I/I_o = s^2/(e + (e^2 - s^2)^{\frac{1}{2}})^2 \end{aligned} \qquad (10)$$

A plot of I/I_o as a function of e/s implies a symmetrical Bragg reflection from a thick crystal with negligible absorption. The reflection is symmetric about the corrected Bragg angle θ_o. In the middle region there is perfect reflection over a width 2s (see Fig. 2).

The full width at half maximum is the range over which I is greater than half the maximum intensity I_o. Taking into account the wings, that range is

$$e/s = 2.12 \qquad (11)$$

From our parameterization

$$e = \theta - \theta_o = \Delta\theta \qquad (12)$$

then the full angular width of the curve at half maximum intensity is

Figure 2. Darwin reflection curve. The ideal curve neglects absorption.

FIGURE 2

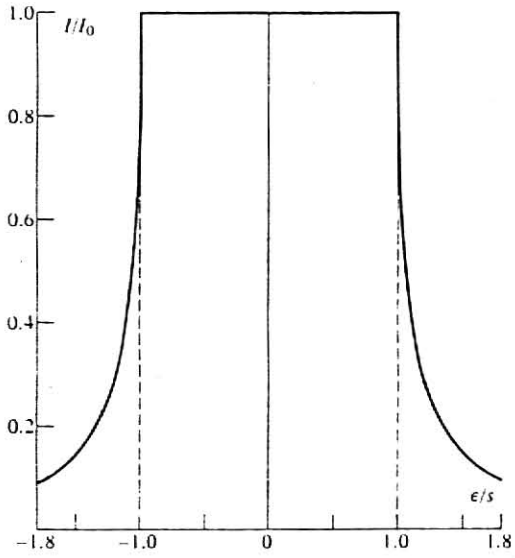

$$\theta_{FWHM} = w_{\frac{1}{2}} = 2.12\ s \quad . \tag{13}$$

If an unpolarized primary beam is assumed, we must multiply s by the polarization factor $(1 + |\cos 2\theta|)/2$. Then

$$s = (e^2/mc^2)N\lambda^2 F(2\theta)/\pi \sin 2\theta\ (1 + |\cos 2\theta|)/2 \tag{14}$$

which can be used to obtain a theoretical value for θ_{FWHM}.

This Darwin curve cannot be observed directly since dispersion of the x-ray beam would wash out a curve typically only a few seconds wide. However, the double crystal spectrometer in the parallel (1,-1) position lends itself to the measurement of perfect crystal reflection widths since it has no dispersion. This means that if λ_1 and λ_2 are being reflected from crystal A, the reflected beams will fall on crystal B at the same respective angles in the (1,-1) position (see Fig. 3). Then if the second crystal B is rotated through an angle θ_B, the intensity at the detector as a function of the angle θ_B is independent of the wavelength and depends only on the convolution of the reflecting power widths of the two crystals. This intensity verses θ_B curve is called the rocking curve.

The mathematical expression for this convolution is of the form

$$R(\theta) = k \int_{-\infty}^{\infty} R_A(\theta_A)\ R_B(\theta - \theta_B)\ d\theta \tag{15}$$

Figure 3. Schematic diagram of the double crystal spectrometer in the parallel (1,-1) position.

FIGURE 3

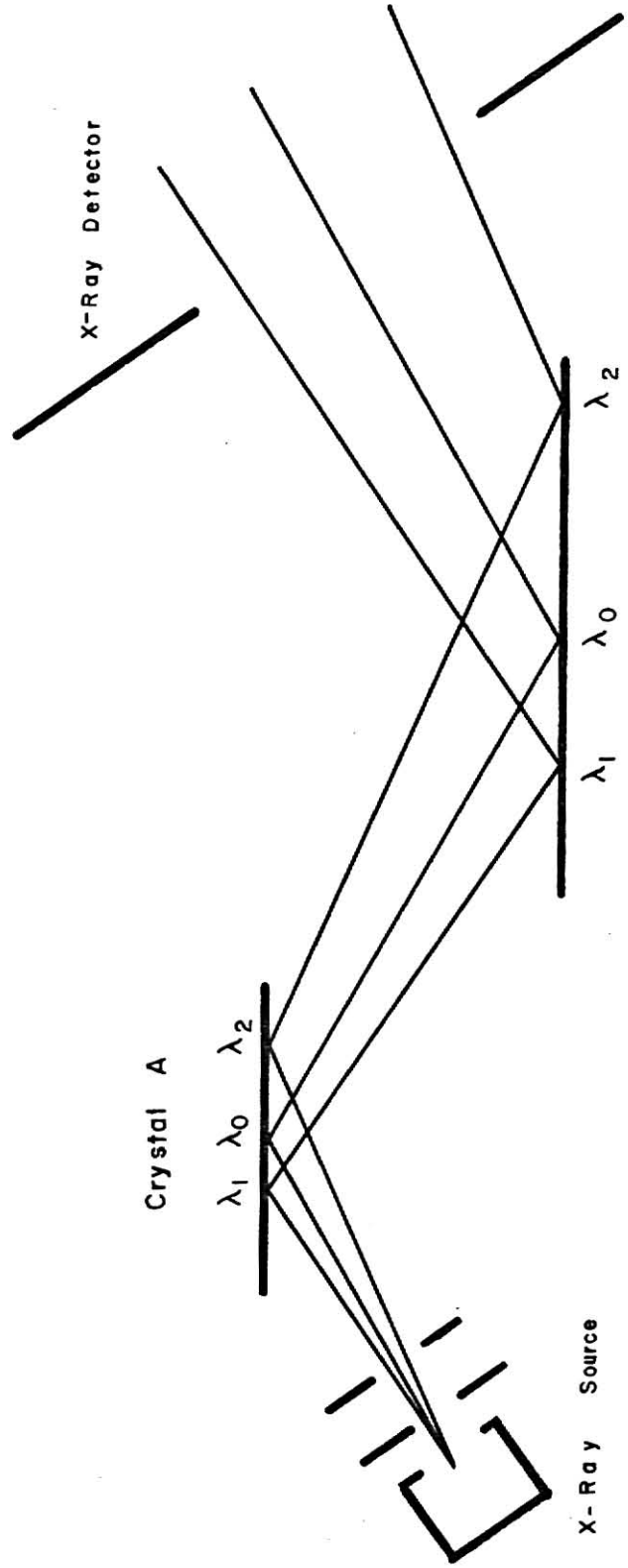
X-Ray Detector
Crystal A
λ_2
λ_0
λ_1
Crystal B
λ_2
λ_0
λ_1
X-Ray Source

where k is a normalization constant, $R_A(\theta_A)$ is the reflection coefficient of the first crystal which is fixed at the Bragg angle and $R_B(\theta - \theta_B)$ is the reflection coefficient of the second crystal which is rocked through the angle θ with respect to the beam incident from crystal A.

As is indicated in Fig. 4, the convolution operation can be thought of graphically as being separated into four basic operations: folding, displacement, multiplication, and integration. In terms of the convolution of the crystals A and B, folding consists of taking the mirror image of $R_B(\theta_B)$ about the ordinate axis. Displacement consists of shifting $R_B(-\theta_B)$ by the amount θ. Multiplication is the product of the shifted function $R_B(\theta - \theta_B)$ and $R_A(\theta_A)$. Integration interprets the area under the product as the value of the convolution at the angle θ. The resulting curve is called the rocking curve. Figure 5 illustrates how the convolution of two step functions of equal width but unequal amplitude yields such a curve. It is apparent that the value of the integral is appreciable only when the curves overlap. In the case of the double crystal spectrometer in the (1,-1) position, the rocking curve is a maximum when $\theta_A = \theta_B$, i.e. when the crystal faces are parallel.

In order to compare the rocking curve with the predicted single reflection curves, we must consider how the full width at half maximum of the observed rocking curve, w_s, is related to the corresponding width of the reflection curve for the

Figure 4. Graphical interpretation of convolution.

(a) Two functions to be convoluted.

(b) Taking the mirror image of each of the given functions about the ordinate axis.

(c) Shifting each of the folded functions by the amount t.

(d) Multiplying the shifted function by the function directly above it in (a).

(e) Interpretation of the area under the product as the value of the convolution at t.

FIGURE 4

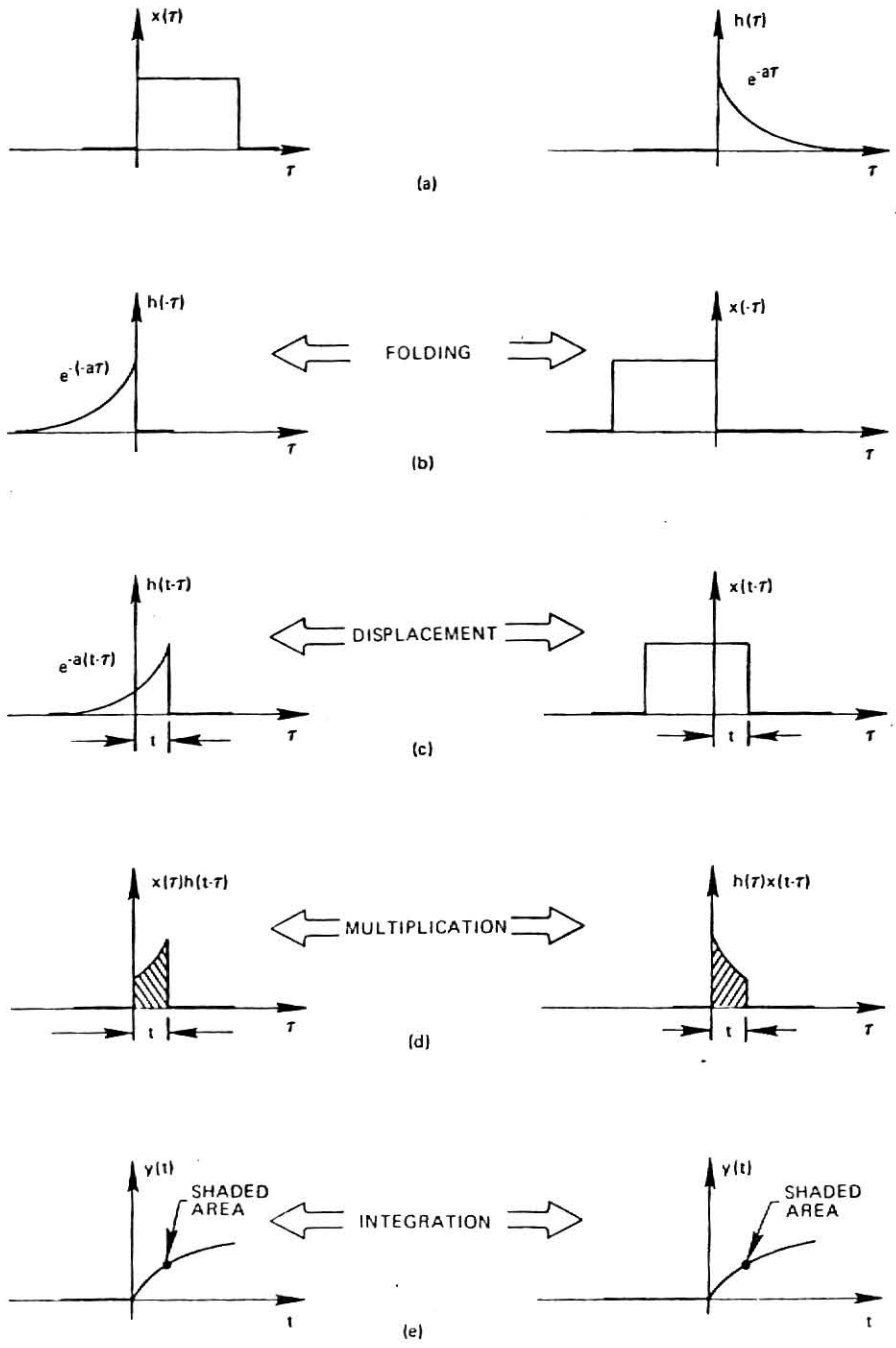
x(τ)
τ
h(τ)
e^-aτ
τ
(a)
h(-τ)
e^-(-aτ)
τ
FOLDING
x(-τ)
τ
(b)
h(t-τ)
e^-a(t-τ)
t
τ
DISPLACEMENT
x(t-τ)
t
τ
(c)
x(τ)h(t-τ)
t
τ
MULTIPLICATION
h(τ)x(t-τ)
t
τ
(d)
y(t)
SHADED AREA
t
INTEGRATION
y(t)
SHADED AREA
t
(e)

Figure 5. Graphical interpretation of the convolution of step functions.

FIGURE 5

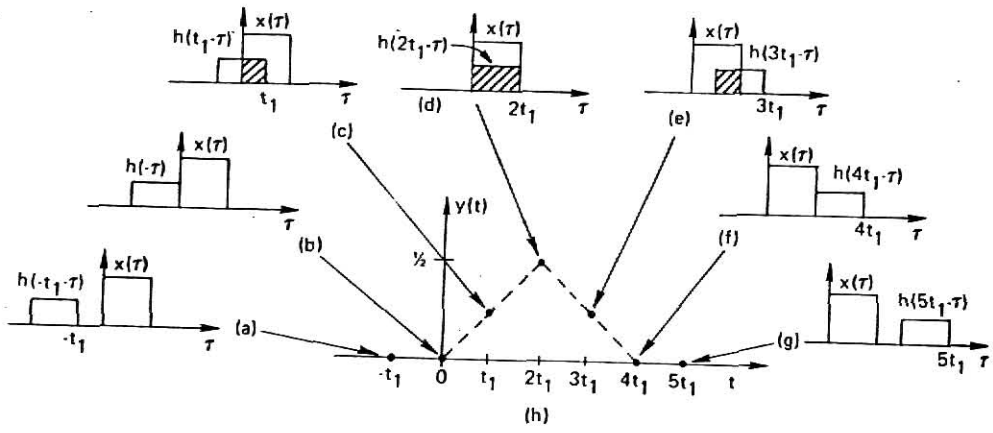
h(t1-τ)
x(τ)
t1
τ
h(2t1-τ)
x(τ)
(d)
2t1
τ
x(τ)
h(3t1-τ)
(e)
3t1
τ
(c)
h(·τ)
x(τ)
τ
y(t)
(b)
½
x(τ)
h(4t1-τ)
4t1
τ
(f)
h(-t1-τ)
x(τ)
-t1
τ
(a)
-t1
0
t1
2t1
3t1
4t1
5t1
t
(h)
(g)
x(τ)
h(5t1-τ)
5t1
τ

single crystal, w_c. No general relation can be given since the width depends on the specific form of R_A and R_B. The width w_s is usually thirty to forty percent greater than w_c.

The convolution of the Darwin shaped curves of Fig. 6 gives $w_s = 1.32\ w_c$. The Gaussian curve convolution gives a Gaussian width of $w_s = \sqrt{2}\ w_c$. Note that it is possible for the convolution to be symmetric where the single reflection curves are not. The best that can be done in comparing experiment and theory is to assume some form for R_A and R_B, calculate the corresponding convolution and compare it with observation.

In an experimental arrangement, such things as slit edges and absorption enter into the convolution process in a way as to round the corners of the ideal Darwin reflection curve. It is for this reason that a Gaussian form for R_A and R_B has been assumed for this research. Also, the Gaussian curves lend themselves to a relatively simple mathematical characterization of the FWHM of a crystal reflection.

ION IMPLANTATION

An energetic ion, upon entering a thick crystal will lose energy first by elastic electronic collision and finally by inelastic nuclear collision with atoms of the host solid. The ion will travel a distance R, called the range, in the host crystal and come to rest a distance R_p from the surface

Figure 6. The relation between the FWHM of single and double reflection curves for different assumed form of the single reflection curve. The solid line represents single reflection curves and the dotted line represents the convolution with itself. a) Step function; b) Sawtooth; c) Darwin shape; d) Gaussian shape.

FIGURE 6

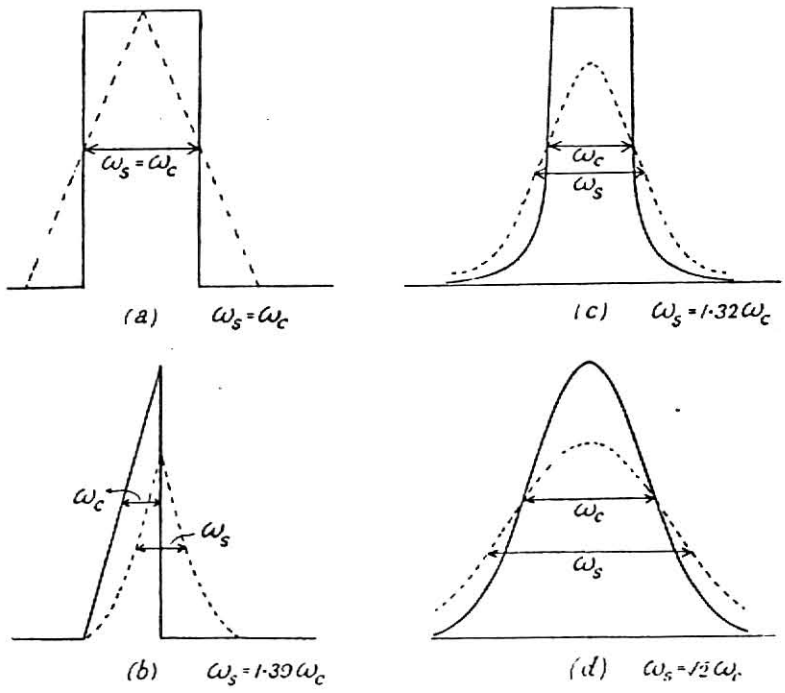
$\omega_s = \omega_c$
(a) $\omega_s = \omega_c$
ω_c
ω_s
(c) $\omega_s = 1.32\omega_c$
ω_c
ω_s
(b) $\omega_s = 1.39\omega_c$
ω_c
ω_s
(d) $\omega_s = \sqrt{2}\omega_c$

of the crystal. The projected range, R_p, must be described statistically in an amorphous solid since the energy lost per collision and the number of collisions are random variables. A well developed theory by Lindhard, Scharrf and Schiott[16], called the LSS theory, uses a statistical amorphous model to express the projected range of ions in a solid in terms of a projected standard deviation about a mean projected range.

Unfortunately the problem of range distributions in single crystals is not well developed. The problem here is that if low index crystallographic planes lie close to the incident beam direction, many of the particles will penetrate to an extraordinary depth. This is called channeling.[17]

Qualitatively, the range distributions in crystals often exhibit two peaks. One peak is due to ions which strike the surface close to an atom and are widely deflected. The regularity of the crystal lattice is lost to these ions and they are stopped as in an amorphous material. The second peak is due to ions which strike the surface of the host crystal at an "open" spot and are deflected only slightly and enter the crystal along a "channel."

These range statistics give information on the shallow peak even if channeling is an important process. The mean projected range of Argon and Rubidium into MgO was calculated by R. D. Dragsdorf[18] of Kansas State University using a computerized version of the LSS model and found the range to be 356 Å for 60 keV Argon ions and 213 Å for Rubidium ions of

the same energy. The standard deviation about this mean projected range was found to be 86 Å and 35 Å for Argon and Rubidium ions, respectively. Calculations of the absorption of x-rays by MgO indicate that the intensity is attenuated to a value of 1/2 its initial intensity in a distance of 69 μm. Thus the implanted region is well within the range of x-ray penetration.

IMPLICATION OF A LARGER FWHM

One might imagine an experiment in which a crystal is set in an x-ray beam at the Bragg angle and a second identical crystal is placed in the reflected beam of the first. If the second crystal were rocked through the Bragg angle and an ionization detector were placed in an appropriate position to detect the x-ray intensity from the second crystal, an intensity verses angle graph could be plotted and the single crystal widths compared with theory.

One might ask how the rocking curve would be modified if the second crystal were implanted with ions. One might suspect that, on the average, the normal lattice would be compressed on one side of the ion distribution and expanded on the side of the incident ion beam if the ions were to kick the host atoms into interstitial positions. The effect of this on the diffraction of x-rays would be to shift the diffracted beam to a slightly higher angle for the compressed

region and shift the diffracted beam to a slightly lower angle for the expanded region. The single crystal width for this crystal would be increased and the convolution with the undamaged first crystal would exihibit a larger FWHM.

Assuming Gaussian shapes, one may express the reflection coefficient of the first crystal as

$$R_A = A\ e^{-ax_{\frac{1}{2}}^2} \tag{16}$$

where A is the maximum reflection from crystal A, a is related to the FWHM of the first crystal reflection curve, and $x_{\frac{1}{2}}$ is the half width at half maximum of the Gaussian curve. Likewise, one may express the reflection coefficient of the second crystal as

$$R_B = B\ e^{-bx_{\frac{1}{2}}^2} \tag{17}$$

where B is the maximum reflection from crystal B and b is related to the FWHM of the second crystal reflection curve. Then the convolution of R_A and R_B yields a Gaussian curve whose FWHM is given by

$$w_{\frac{1}{2}} = 2((a + b)/(ab)\ \ln\ 2)^{\frac{1}{2}} \quad . \tag{18}$$

If the second crystal has been implanted with ions, one might wish to separate the "natural" width of the single

crystal reflection curve from that part of the reflection curve width due to strain in the crystal caused by the implanted ions.

The width of the unimplanted reflection curve includes such things as the natural width and thermal broadening. We can express this undamaged width in terms of the b's of Eq. 17 as

$$b^2_{\text{unimplanted}} = b^2_{\text{natural width}} + b^2_{\text{thermal}} \quad . \qquad (19)$$

One can characterize the $w_{\frac{1}{2}}$ of the implanted crystal in a similar manner as

$$b^2_{\text{implanted}} = b^2_{\text{strain}} + b^2_{\text{unimplanted}} \; ; \; b_{\text{unimp.}} = a \qquad (20)$$

Substituting $b_{\text{implanted}}$ into Eq. 18, one can relate the b^2_{strain} coefficient to the implanted FWHM, $w_{\frac{1}{2}\text{im}}$, and the unimplanted FWHM, $w^2_{\frac{1}{2}\text{un}}$, as

$$b^2_{\text{strain}} = ((4 \ln 2)/(w^2_{\frac{1}{2}\text{im}} - w^2_{\frac{1}{2}\text{un}}))^2 - ((4 \ln 2)/(w^2_{\frac{1}{2}\text{un}})).^2 \qquad (21)$$

The strain coefficient may be related to the strain by partial differentiation of Braggs law, first with respect to d, then with respect to θ. Dividing by Braggs law it is found that

$$\text{Strain} = \Delta d/d = -\cot\theta\ \Delta\theta \tag{22}$$

where $\Delta\theta$ may be related to the unimplanted and implanted rocking curve widths as

$$w^2_{\frac{1}{2}im} = w^2_{\frac{1}{2}un} + (\Delta\theta)^2. \tag{23}$$

Substituting from Eq. 23 into Eq. 22, a direct relation between the b coefficients and the strain can be obtained as

$$\Delta d/d = ((b_{st}/(4\ \ln\ 2))^2 + (1/w_{\frac{1}{2}un})^2)^{-\frac{1}{4}}\ \cot\theta\ . \tag{24}$$

Substituting for $\Delta\theta$ in Eq. 22 from Eq. 23, the strain can be expressed in terms of $w^2_{\frac{1}{2}im}$ and $w^2_{\frac{1}{2}un}$ as

$$\text{Strain} = \Delta d/d = -\cot\theta\ (w^2_{\frac{1}{2}im} - w^2_{\frac{1}{2}un})^{\frac{1}{2}}\ . \tag{25}$$

THE EXPERIMENT

DESCRIPTION OF THE APPARATUS

The double crystal spectrometer used in this experiment was constructed at Kansas State University and was used in conjunction with a General Electric XRD-6 x-ray tube power supply and a General Electric SPG-4 detection system consisting of a pulse height analyzer, a scaler counting unit, a counting ratemeter and a high voltage power supply for the General Electric SPG-10 proportional counter which was operated at 1500 volts throughout the experiment.

Copper K_α radiation was used in the experiment with the tube operated full wave rectified at 35 kilovolts and a tube current of 18 milliamperes.

A photograph of the spectrometer is shown in top view of Plate 1 and in side view in Plates 2 and 3. K_{α_1} radiation from the Cu tube (λ = 1.542 Å) was incident onto the first crystal mounted at turntable A. Turntable A was rotatable through 360 degrees. The crystal holder, mounted on turntable A, allows the crystal to be translated perpendicularly to the axis of rotation of the turntable. This crystal holder may be tilted slightly with respect to the vertical in order to bring the crystal face parallel with the vertical beam incident from the x-ray tube through two vertical slits. This adjustment allows the reflected intensity to be maximized and does not affect the shape of the reflection curve. The K_{α_1} and

Plate 1. Top view of double crystal spectrometer.

THIS BOOK CONTAINS NUMEROUS PAGES WITH PICTURES THAT ARE CROOKED COMPARED TO THE REST OF THE INFORMATION ON THE PAGE.

THIS IS AS RECEIVED FROM CUSTOMER.

THIS BOOK CONTAINS SEVERAL DOCUMENTS THAT ARE OF POOR QUALITY DUE TO BEING A PHOTOCOPY OF A PHOTO.

THIS IS AS RECEIVED FROM CUSTOMER.

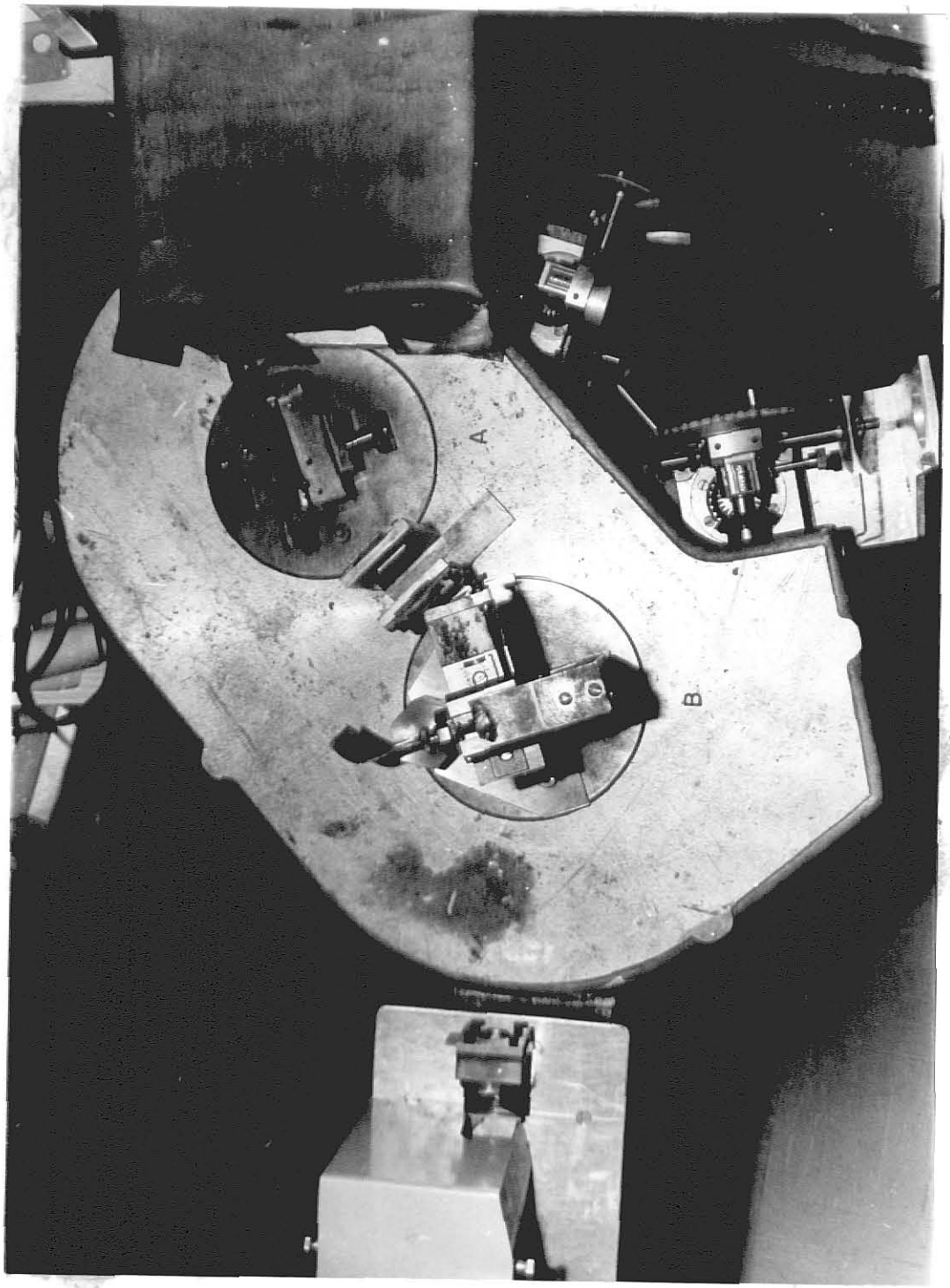

PLATE I

Plate 2. Two side views of the double crystal spectrometer.

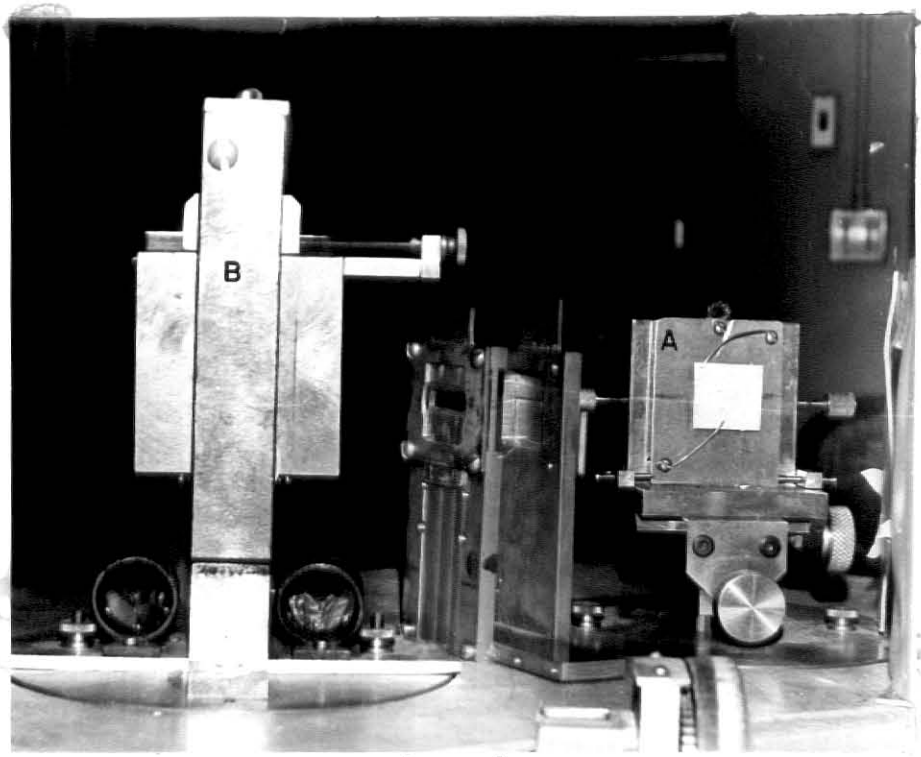

(a)

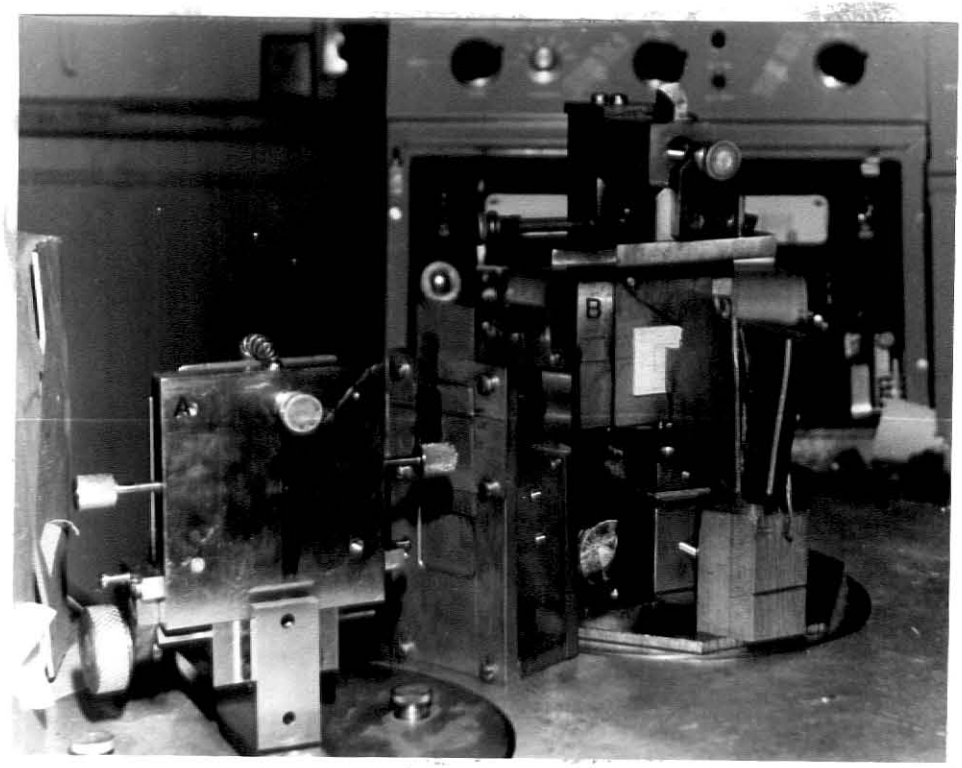

(b)

PLATE 2

K_{α_2} radiation is diffracted from the first crystal at slightly different angles. A vertical lead shield is necessary to eliminate the K_{α_2} radiation. This vertical shield is attached to the first of two movable horizontal collimation slits placed approximately midway between turntable A and turntable B. The slit holder rests on the steel housing of the spectrometer. Turntable B is also rotatable through 360 degrees by means of gears concealed under the steel housing.

The crystal mount of turntable B is translatable both parallel and perpendicular to the beam from crystal A and will tilt with respect to the vertical to allow the second crystal to be vertically aligned parallel with the first. A lead beam stop is placed close to the face of the second crystal to eliminate direct and scattered x-ray radiation. A relatively wide vertical slit in front of the x-ray detector also helps to eliminate this problem. The whole steel housing is rotatable about the turntable A. The x-ray detector rotates coaxially with turntable B.

ALIGNMENT PROCEDURE

With the x-rays on and the x-ray counter in the direct beam, the horizontal slit system was inserted into the beam and adjusted by moving the slits up or down until the correct height was obtained. This was indicated by a maximum reading on the counting ratemeter. This procedure adjusted the

intermediate slit system to the height of the beam.

With the first crystal in a nearly vertical position, the horizontal slits were removed and the first crystal was rotated so its face was approximately parallel to the beam from the x-ray tube. The crystal was then translated into the beam until the ratemeter indicated an intensity which was half the initial intensity. Again the crystal was translated perpendicular to the beam until half the initial intensity was again indicated on the ratemeter. This procedure was repeated until a rotation of the crystal produced only an attenuation of the beam and the beam intensity was half the beam intensity directly from the x-ray tube. This procedure centered the face of the crystal about a vertical axis at the center of rotation of turntable A and aligns the crystal face parallel to the beam.

With the second crystal mount removed, the first crystal was rotated through its Bragg angle while the x-ray detector was rotated through an angle twice the Bragg angle until the first order diffraction intensity was observed. The K_β line is close to the K_α line and appears at a significantly lower intensity and at a smaller angle than the K_α. The intensity of the K_α was maximized by adjusting the rotational position of both the crystal and x-ray detector.

The tilt of the first crystal was adjusted alternately with the rotation angle to obtain the maximum intensity at the x-ray detector. The initial alignment procedure for the first crystal was then repeated to insure that the face of the

crystal was at the center of rotation of turntable A.

With a small pin positioned at the center of rotation of turntable B, the entire steel housing was rotated about the turntable A until the beam was positioned at the center of rotation of turntable B. Rotation of crystal A and the x-ray detector was necessary to maintain the proper Bragg angle. The correct rough positioning of the beam at the center of rotation was indicated by its attenuation by the small pin.

The horizontal slit system was placed midway between turntable A and turntable B with the vertical shield intercepting the K_{α_2} beam on the low angle side. It was found that an attenuation of the beam of one fourth its original intensity insured that the K_{α_2} radiation was intercepted. The housing was rotated about turntable A as before until the K_{α_2} beam was completely intercepted by the pin and a maximum intensity obtained when the pin was removed. This procedure positioned the K_{α_1} beam at the center of rotation of turntable B and removed the K_{α_2} component from the beam. The intensity from crystal A was then maximized by fine adjustments of rotation and tilt angle and were subsequently left in this position throughout the remaining experimental trials.

The second crystal holder was mounted on turntable B and rotated so that the crystal was approximately parallel to the beam incident from crystal A. With the detector in the beam, the second crystal was translated into the beam until the intensity was attenuated to half its original value. This crystal was then rotated in such a manner that an increase in

intensity was indicated on the ratemeter. This crystal was alternately rotated and translated in a manner analogous to the first crystal until its face was parallel to the beam and at the center of rotation of turntable B.

The crystal B was then rotated through the Bragg angle while the detector was translated through twice the Bragg angle. The intensity from this crystal was maximized by alternately adjusting the rotation angle of the crystal and detector and the tilt of the crystal. The second crystal was then rotated to its original position parallel to the beam and the crystal face was repositioned as before to assure that the tilt adjustment did not move the crystal face from the center of rotation of turntable B. The second crystal was then again rotated through its Bragg angle and fine adjustments of tilt and rotation made to achieve a maximum intensity at the detector. At this point the second crystal should be exactly parallel with the first. The lead beam stop was then placed at the face of the second crystal at the point where the beam hit the crystal. All rocking curves were taken from higher to lower angle.

CALIBRATION

Although the spectrometer gears were designed to indicate the angular displacement of crystal B to fractions of a second, it was found that backlash and imperfections in the gears

prevented this accuracy. Since the theoretical widths of the crystals used were on the order of seconds, another method for measuring this angle was required.

A traveling microscope-laser system was devised to calibrate the angle measuring system of the spectrometer. A high order diffraction fringe from a slit used in conjunction with a Metrologic He-Ne laser was reflected from a front surface mirror fixed at the top of the second crystal mount onto the objective of a traveling microscope with a crosshair eyepiece. As the second crystal was rotated, the traveling microscope followed a single order of diffraction. The microscope movement closely approximated the arc length as the distance from the objective to the mirror was large compared to the small motion of the fringes. With this system, angles of five seconds were easy to measure. With smaller angles the limiting factor was the ability to place accurately the crosshair on a fringe and the ability to read the microscope micrometer.

LINEARITY CHECK

At the beginning of the experiment the linearity of the x-ray counting system was checked. One mil thicknesses of aluminum foil were placed in front of the detector and the number of counts recorded for a time interval of ten seconds. Every tenth pulse was counted yielding a count rate in counts per second.

The absorption follows Beer's law;

$$I = I_o e^{-u_1 nt} \tag{26}$$

where u_1 is the linear absorption coefficient, I_o is the intensity of the incident beam, I is the intensity of the attenuated beam, t is the thickness of an aluminum sheet and n is the number of aluminum sheets.

The natural logarithm of the ratio of the incident intensity, I_o, to the transmitted intensity, I, was plotted against the number of thicknesses of aluminum foil in Fig. 7. The linear absorption coefficient may be derived from the slope of this line. For aluminum, u_1 was calculated to be 131 (cm^{-1}). A least squares fit to the line yielded a linear absorption coefficient of 153 (cm^{-1}) with a regression constant of 0.9995. The y intercept was computed to be -0.06. The deviation from the theoretical value could arise if the foil were composed of an aluminum alloy rather than pure aluminum. However the counting system is linear up to counting rates of 1,000 counts per second.

CALCITE

In order to assure proper operation of the double crystal spectrometer and to develop a technique in the use of the spectrometer, rocking curves for two naturally occurring calcite crystals were taken. Both crystals were mounted

Figure 7. X-ray counting system linearity check. The equation of the line is $I/I_o = 0.389\ n - 0.06$.

FIGURE 7

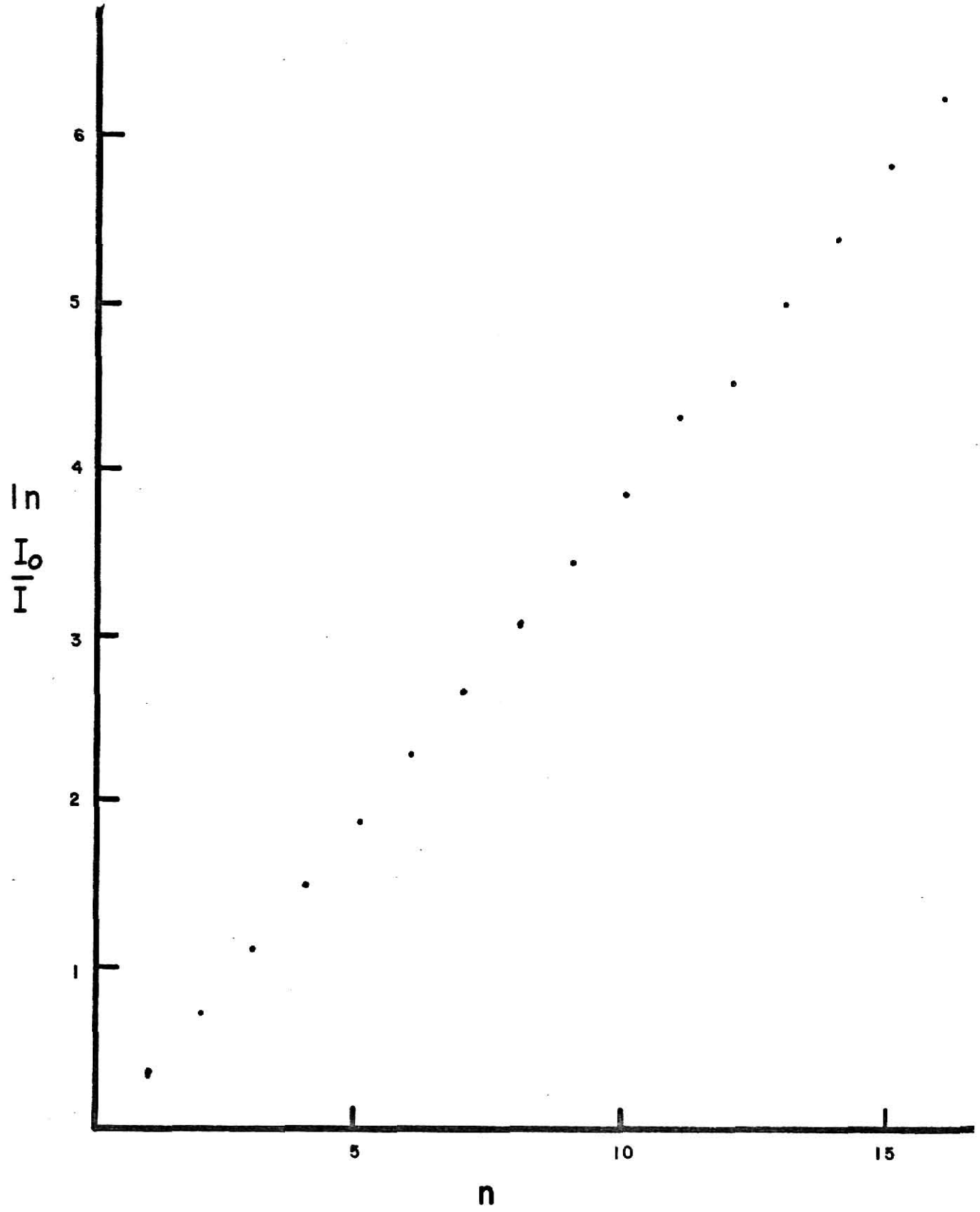

directly to the crystal holders. A crystal marked "B and L" was used as a monochromating crystal and the analyzing crystal was marked "Bill." Both crystals were obtained from J. Bearden[19] of The John Hopkins University. The first rocking curves taken with these crystals exhibited widths of twenty to thirty divisions. Upon etching both crystals in a solution of one part distilled H_2O to ten parts 12 M HCL[20] for approximately ten seconds at room temperature, they were examined under the microscope and revealed a clean, etched surface. Subsequent rocking curves revealed a FWHM of 10.5 seconds (see Fig. 8). The calibration curve shown in Fig. 9 is the result of examining laser fringes as previously discussed. It exhibits a slope of 0.0017 ± 0.0008 in./10 divisions. This conversion in terms of seconds of arc is 10 divisions = 1.0 ± 0.5 seconds. Then the FWHM of the calcite rocking curve is within the 10.7 seconds predicted by the Darwin theory. Thus the spectrometer has correctly reproduced the theoretical results.

A plotting program was used in conjunction with the HP-9600 programable calculator and plotter. This consisted of a scale drawing program and a plotting program. The scale drawing program is entered on the positive page of the calculator and the plotting program entered on the negative page. Listings of both programs appear in Fig. 10.

To use the scale drawing program:

1. Enter the y scale factor (y = 4500/maximum intensity) into "a".

Figure 8. Rocking curve of calcite. The FWHM is 10.5 ± 0.5 seconds. The Darwin theory predicts a value of 10.7 seconds.

FIGURE 8

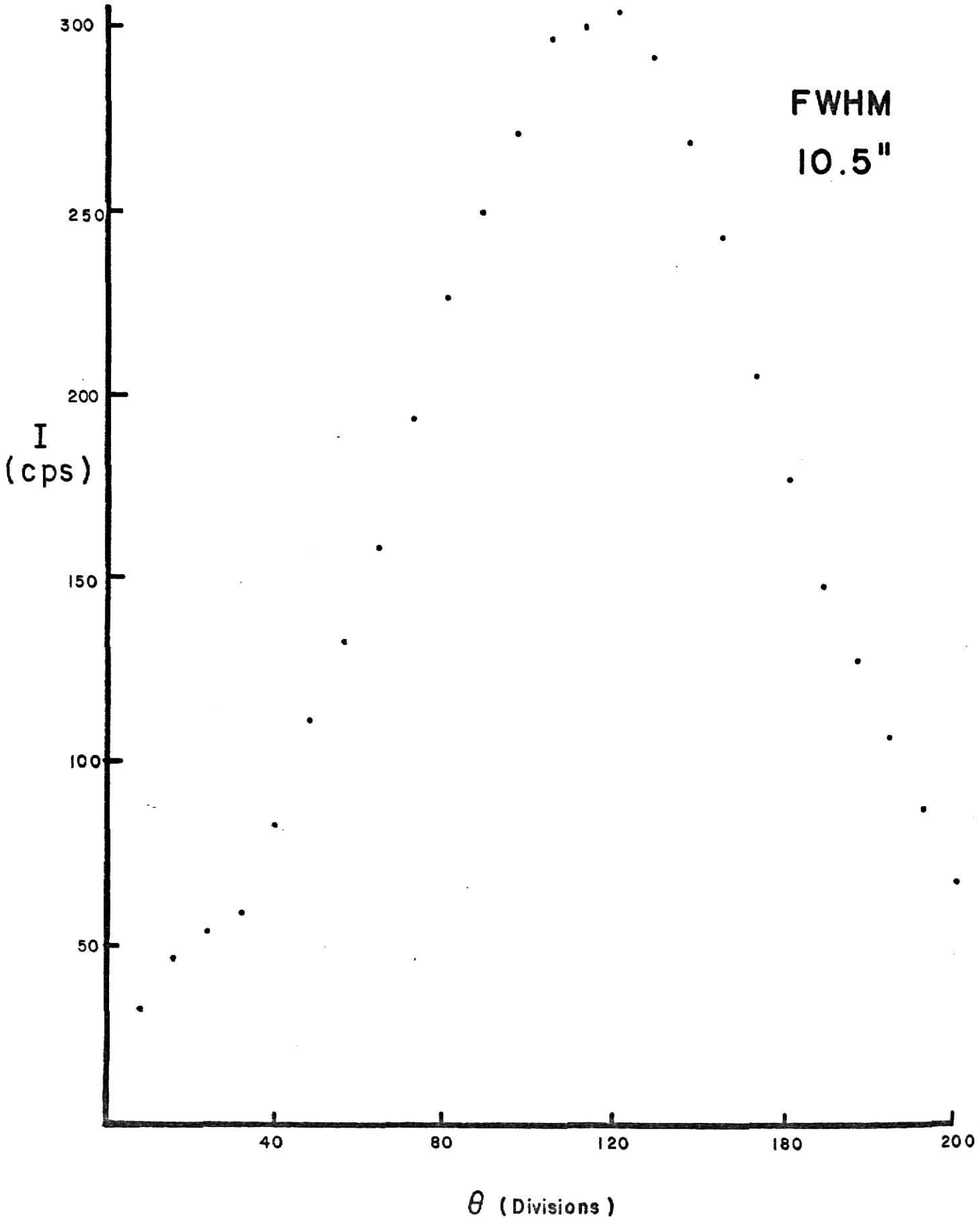
FWHM
10.5"
I
(cps)
300
250
200
150
100
50
40
80
120
180
200
θ (Divisions)

Figure 9. Double crystal spectrometer angle calibration for calcite. 1.0 second = 1 division.

FIGURE 9

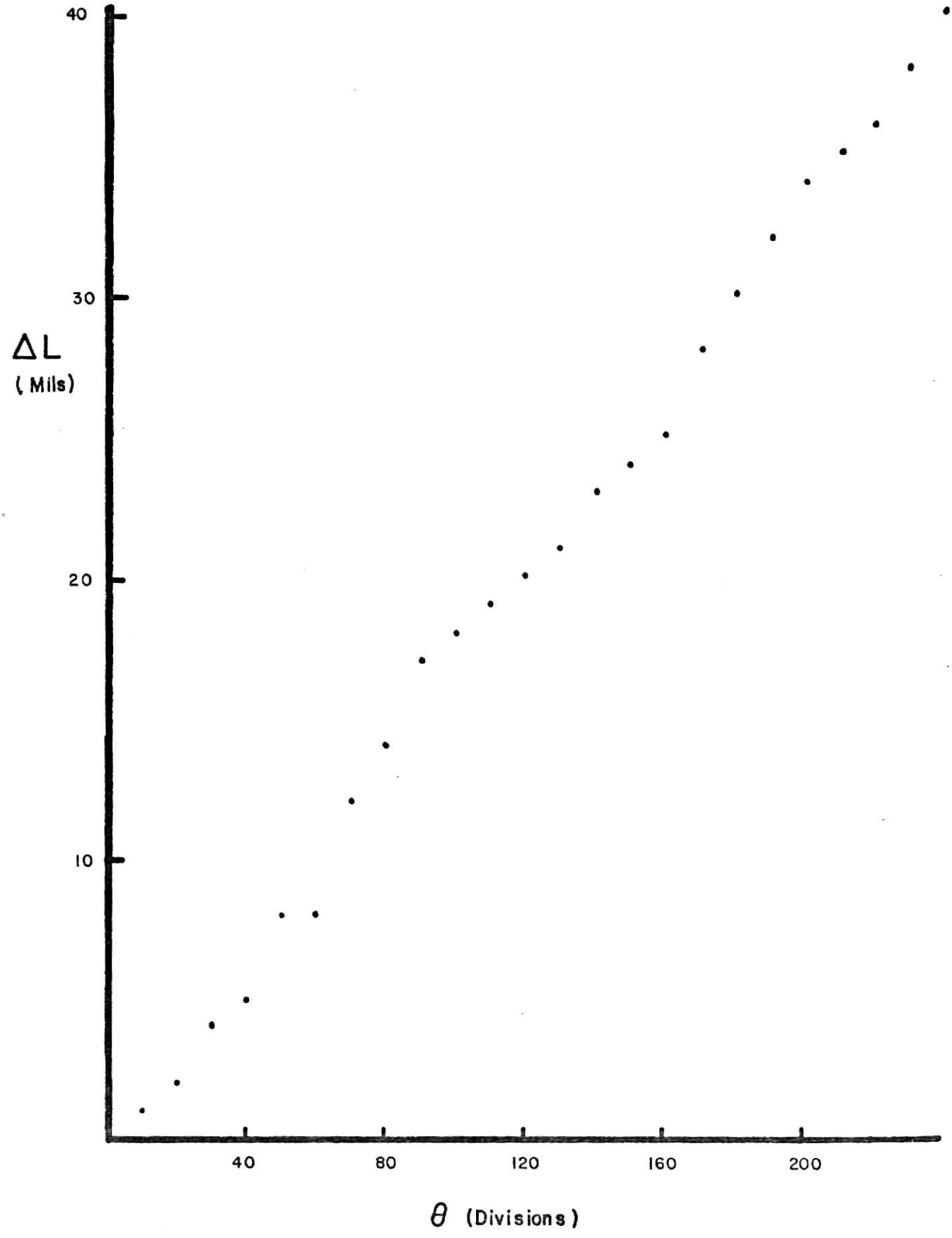

Figure 10. Plotting program and scale drawing program for Hewlett-Packard 9600 programable calculator. Scale drawing program is on the positive page and the plotting program is on the negative page.

FIGURE 10

Step Number	Step	Step Number	Step	Step Number	Step	Step Number	Step
0.0	00	3.0	43	6.0	44	9.0	04
0.1	27	3.1	03	6.1	07	9.1	14
0.2	42	3.2	14	6.2	01	9.2	53
0.3	25	3.3	30	6.3	47	9.3	04
0.4	41	3.4	42	6.4	42	9.4	14
0.5	22	3.5	25	6.5	25	9.5	30
0.6	43	3.6	30	6.6	16	9.6	44
0.7	01	3.7	44	6.7	42	9.7	07
0.8	00	3.8	04	6.8	25	9.8	10
0.9	14	3.9	00	6.9	00	9.9	41
0.a	44	3.a	47	6.a	47		
0.b	01	3.b	42	6.b	47		
0.c	02	3.c	25	6.c	42		
0.d	47	3.d	54	6.d	25		
1.0	13	4.0	25	7.0	54	-0.0	41
1.1	54	4.1	53	7.1	27	-0.1	27
1.2	23	4.2	04	7.2	25	-0.2	13
1.3	34	4.3	14	7.3	17	-0.3	36
1.4	13	4.4	27	7.4	33	-0.4	12
1.5	36	4.5	12	7.5	40	-0.5	22
1.6	40	4.6	33	7.6	15	-0.6	14
1.7	33	4.7	44	7.7	25	-0.7	36
1.8	17	4.8	02	7.8	12	-0.8	31
1.9	25	4.9	17	7.9	33	-0.9	57
1.a	30	4.a	47	7.a	00	-0.a	42
1.b	35	4.b	00	7.b	43	-0.b	25
1.c	40	4.c	43	7.c	10	-0.c	47
1.d	33	4.d	06	7.d	10	-0.d	47
2.0	12	5.0	04	8.0	30	-1.0	12
2.1	41	5.1	30	8.1	42	-1.1	27
2.2	47	5.2	42	8.2	25	-1.2	17
2.3	47	5.3	25	8.3	30	-1.3	33
2.4	47	5.4	22	8.4	44	-1.4	40
2.5	34	5.5	16	8.5	10	-1.5	12
2.6	67	5.6	30	8.6	14	-1.6	44
2.7	34	5.7	42	8.7	47	-1.7	34
2.8	13	5.8	25	8.8	42	-1.8	00
2.9	36	5.9	30	8.9	25	-1.9	00
2.a	27	5.a	31	8.a	54		
2.b	12	5.b	42	8.b	15		
2.c	30	5.c	25	8.c	30		
2.d	00	5.d	30	8.d	50		

2. Enter the x scale factor (x = 7000/maximum angle) into "b".
3. Enter 50 into "c".

To draw the y scale:

a-1. Set Flag

a-2. Go to + 00

a-3. Continue

a-4. Enter 1 into y register

a-5. Enter number of angular divisions between scales to be drawn

a-6. Continue

a-7. Enter starting points for x and y in their respective registers (usually 0,0)

a-8. Continue

a-9. Stop when scale is sufficiently extended.

To draw x scale:

b-1. Clear

b-2. Go to + 00

b-3. Continue

b-4. Enter 1 into y register

b-5. Enter number of intensity divisions between two scales desired.

b-6. Follow steps a-6 to a-9 above.

To use the plotting program:

c-1. Clear

c-2. Go to - 00

c-3. Enter angle increment in "d"

c-4. Enter first intensity data point

c-5. Continue

c-6. Continue

c-7. Repeat c-4 and c-5 until all data is plotted

c-8. Stop.

Note: The x variable, which corresponds to the angle, is automatically incremented by the amount in "d" as each intensity data point is entered and plotted.

MgO HISTORY AND PREPARATION

The two MgO crystals used in this experiment were obtained from the General Electric Corporation. They were grown by the hydrogen fusion process. The dimensions of the crystals were approximately 1.1 cm by 1.1 cm by 0.06 cm. Half of one side of each crystal was separately implanted with 60 keV ions of Rubidium or Argon. The Rubidium ions were implanted at a dose of 10^{16} cm^{-2} and the Argon ions were implanted at a dose of 1.23×10^{15} cm^{-2} by Dr. James Macdonald using the 200 keV accelerator at Kansas State University. The top half of each crystal was masked to preserve the original crystal lattice. This unimplanted half was used in the experiment as the monochromating crystal in each case.

Both crystals were etched in accordance with the previous experience with calcite. The etching solution consisted of one part 18 M H_2SO_4, one part distilled H_2O, and five parts

of a saturated solution of NH_4Cl.[21] The crystals were etched for approximately one minute and examined under a microscope to insure that the surfaces were clean and properly etched. Besides this etching no other treatment was given to these crystals.

Both crystals were examined under crossed polarizers in an investigation of possible strain inherent in the crystals (see Plates 3 and 4). Strain reveals itself as a light area on the photograph. Notice the strain at the bottom of both crystals near the cracks. The thin diagonal lines running through the main body of the crystals are not strained regions but merely surface steps. Overall the crystals appear to be rather good. The strain caused by the implantation cannot be detected by this method.

TOPOGRAPHS

X-ray reflection topographs were made of both crystals in a further investigation of strains inherent in the main body of the crystals. Cu radiation was monochromated by a calcite crystal. The beam was collimated using a 0.5 meter pipe with a narrow slit at one end (see Plate 5). This beam was incident on the crystal at the Bragg angle. Diffracted radiation fell directly on a photographic film situated parallel to the crystal face. The crystal to film separation was about 5 cm. The crystal and photographic film were translated back and forth by means of a Weissenberg camera

Plate 3. Crossed polarizer photograph of Argon implanted MgO. Light areas around edge indicate strain. Bottom half is implanted.

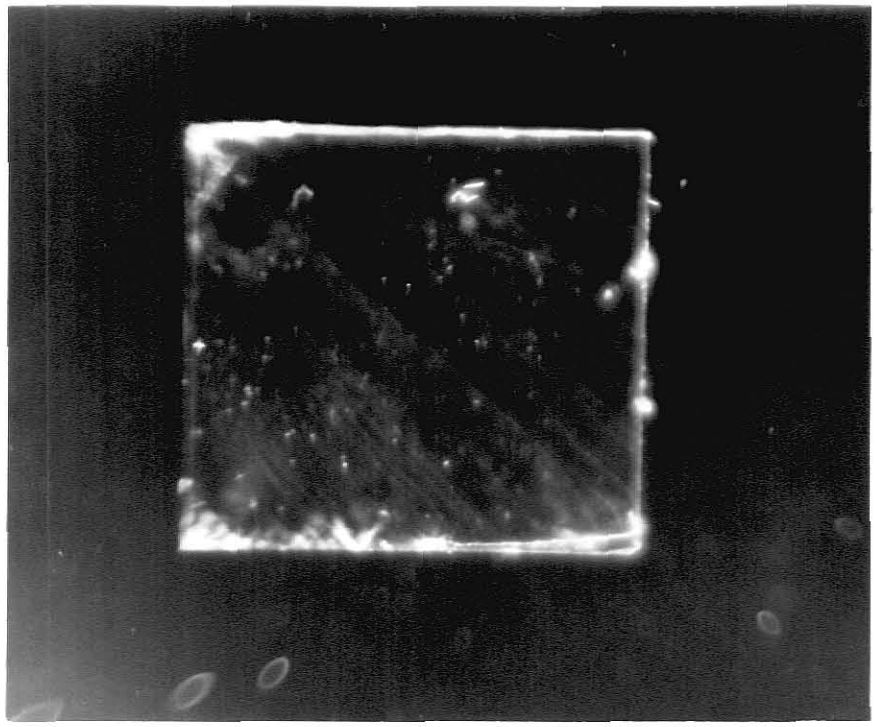

PLATE 3

Plate 4. Crossed polarizer photograph of Rubidium implanted MgO. Light areas around edge indicate strain. Bottom half is implanted.

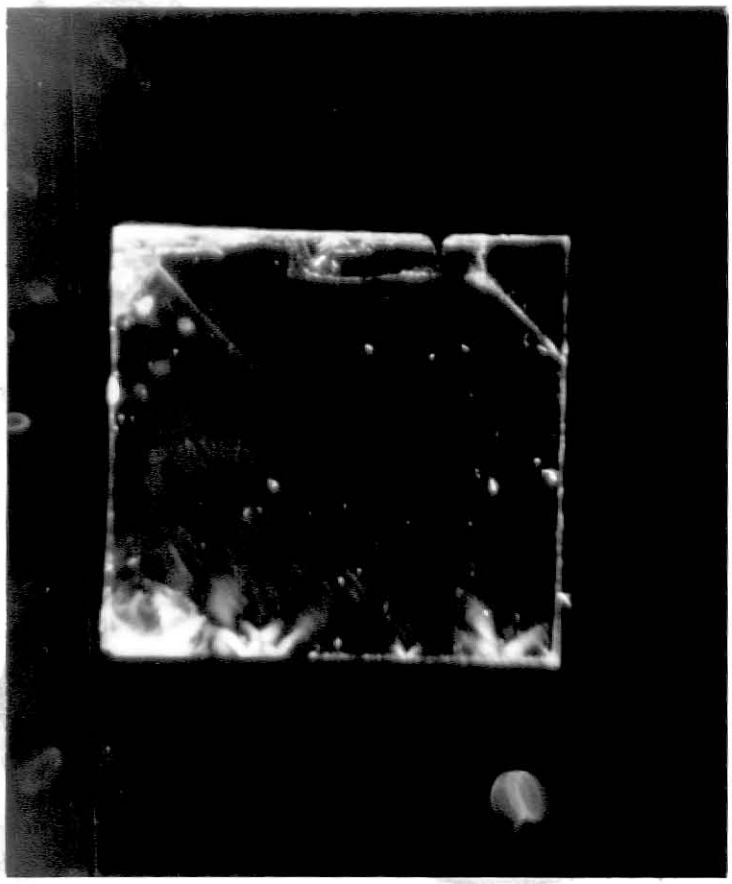

PLATE 4

Plate 5. Weissenberg camera arrangement used to make topographs.

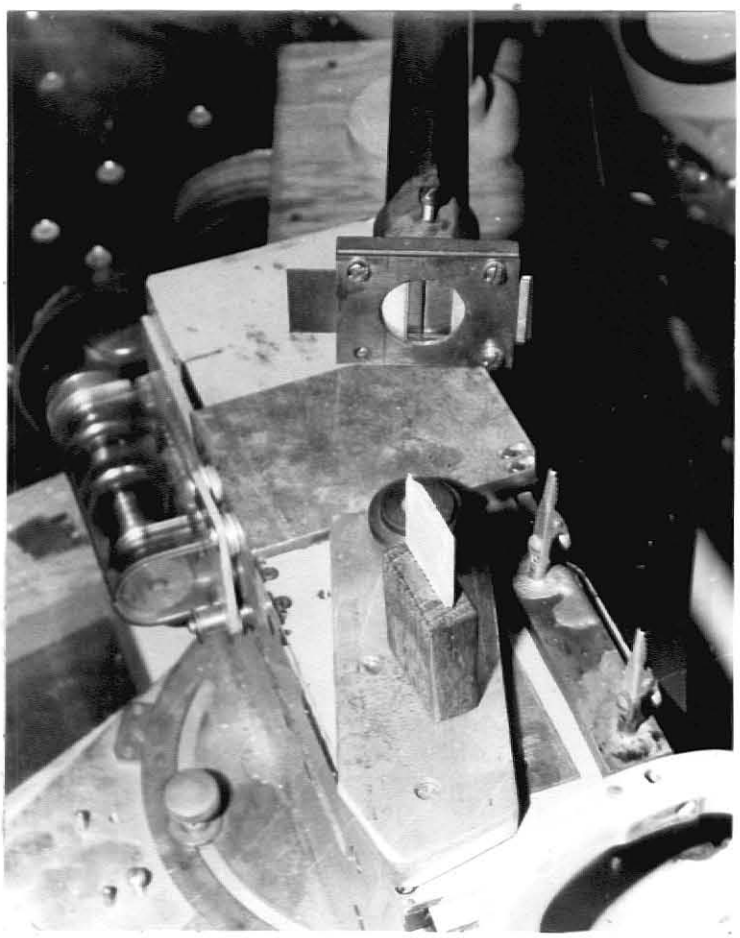

PLATE 5

arrangement, always maintaining the crystal face at the Bragg angle. The Rubidium crystal was exposed for 3.5 hours while the Argon implanted crystal was exposed for four hours in this manner. The Cu tube was run at 35 keV with a tube current of 20 milliamperes. Notice that in the topograph of the Argon implanted crystal the area of implant is apparent (see Plate 6 and 7). Comparison of the topographs, Plates 6 and 7, with the crossed polarizer photos, Plates 3 and 4, reveal strain similarities at the corners and edges of the crystals. The topographs, being sensitive to the d spacing of the crystal, exhibit structure not contained in the crossed polarizer photographs.

THE EXPERIMENT WITH MgO

The Argon and Rubidium crystals were mounted on the spectrometer with the x-ray beam incident on the unimplanted half of each crystal. A series of rocking curves were taken horizontally from one edge of the crystal to the other in approximately one millimeter steps. The crystals were switched and an additional series of curves taken. It was found that both crystals yielded rocking curve half widths on the order of 20 seconds. In one trial a rocking curve width of 13.4 seconds was obtained. Comparing this with the width of 13.3 seconds predicted by the Darwin theory, we see that the unimplanted crystals are rather close to being perfect although there may be some strains inherent as the topographs show.

Plate 6. Topograph of Argon implanted MgO. The bottom half of the crystal is implanted. The area of implant is visible.

PLATE 6

Plate 7. Topograph of Rubidium implanted MgO. The bottom half of the crystal is implanted.

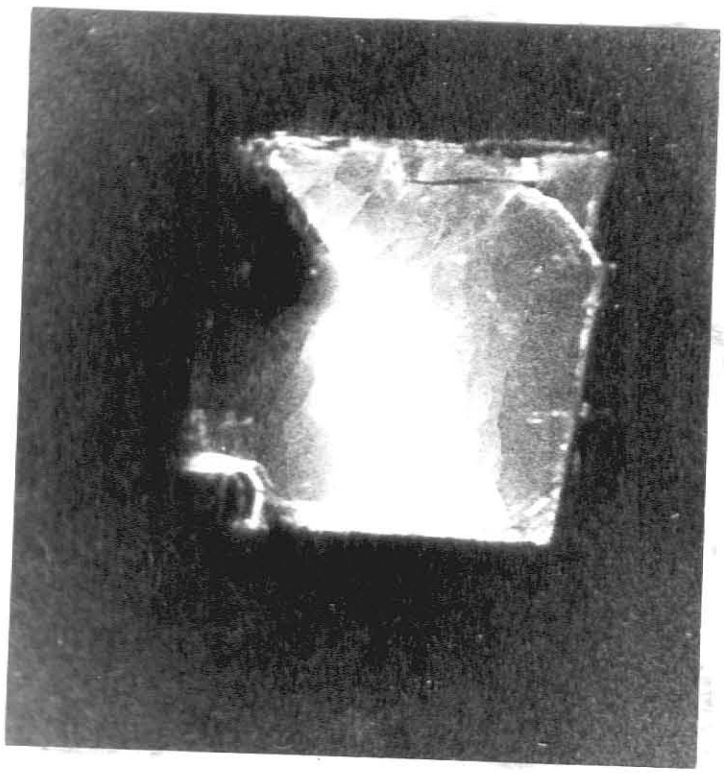

PLATE 7

The unimplanted half of the Argon implanted crystal was used in position A and the implanted half of the Rubidium crystal was used as crystal B. A series of rocking curves were again taken horizontally in the same manner prescribed for the unimplanted curves. The crystals were then switched and another series of rocking curves taken of the Argon implanted crystal.

Both crystals were mounted on balsa wood squares using salol. The balsa wood squares were subsequently mounted on the spectrometer. The balsa should be soft enough to alleviate strain which might be caused by mounting the crystal directly on the spectrometer crystal mounts. The balsa wood squares also provided good thermal insulation to prevent strain which could be caused by thermal gradients in the crystal.

The rocking curves were taken by stepping the second crystal by two division increments. At each position one tenth of the x-ray intensity was counted for a ten second interval. The second crystal was raised by adding washers between the crystal mount foot and foot plate. This insured that x-rays from the same part of the tube struck the second crystal in going from the unimplanted to implanted areas of the second crystal. The necessity of remounting both crystals to make a complete run hampered repeatability. Repeatability was also hampered by the lateral movement of the beam on the crystal due to tilting the second crystal in order to assure proper alignment with the first. This inability to define a

spot on a crystal and to return to a given spot makes it impossible to repeat the experiment in such a way as to reproduce exactly the data given here. Therefore we must settle for looking at the effect due to ion implantation as an average over the face of the crystal.

RESULTS

A typical rocking curve for Rubidium implanted MgO is shown in Fig. 11. This graph exhibits a single peak and is symmetric.

The rocking curve of Fig. 12, with a half width of 13.4 seconds, approaches the theoretical value of 13.3 seconds. While this is not typical of the trials, (in fact this width was never repeated), it does point to the fact that at least one spot on each crystal is very nearly perfect. This is an indication that these crystals are rather good, although not perfect.

The rocking curve of Fig. 13 was taken over a range of 400 divisions either side of the main peak in three division steps. No other peak beside the main peak was observed. This is in contrast to a secondary peak observed by Workman at a lower angle.[22] This is typical of the other rocking curves.

Table I summarizes the rocking curve widths of two runs. These data were taken at the center and edges of each crystal, as indicated in the table. The unimplanted crystal widths were taken with the Argon crystal as the monochromator. The crystal widths taken at the edges of the crystal were taken within two millimeters of the edge.

The calibration curve shown in Fig. 14 was taken in the same angular region as the rocking curves of Table I. A

Figure 11. Typical rocking curve. This particular one is of Rubidium implanted MgO.

ILLEGIBLE

THE FOLLOWING DOCUMENT(S) ARE ILLEGIBLE DUE TO THE PRINTING ON THE ORIGINAL BEING CUT OFF

THIS IS AS RECEIVED FROM THE CUSTOMER AND IS THE BEST POSSIBLE IMAGE AVAILABLE

ILLEGIBLE

FIGURE II

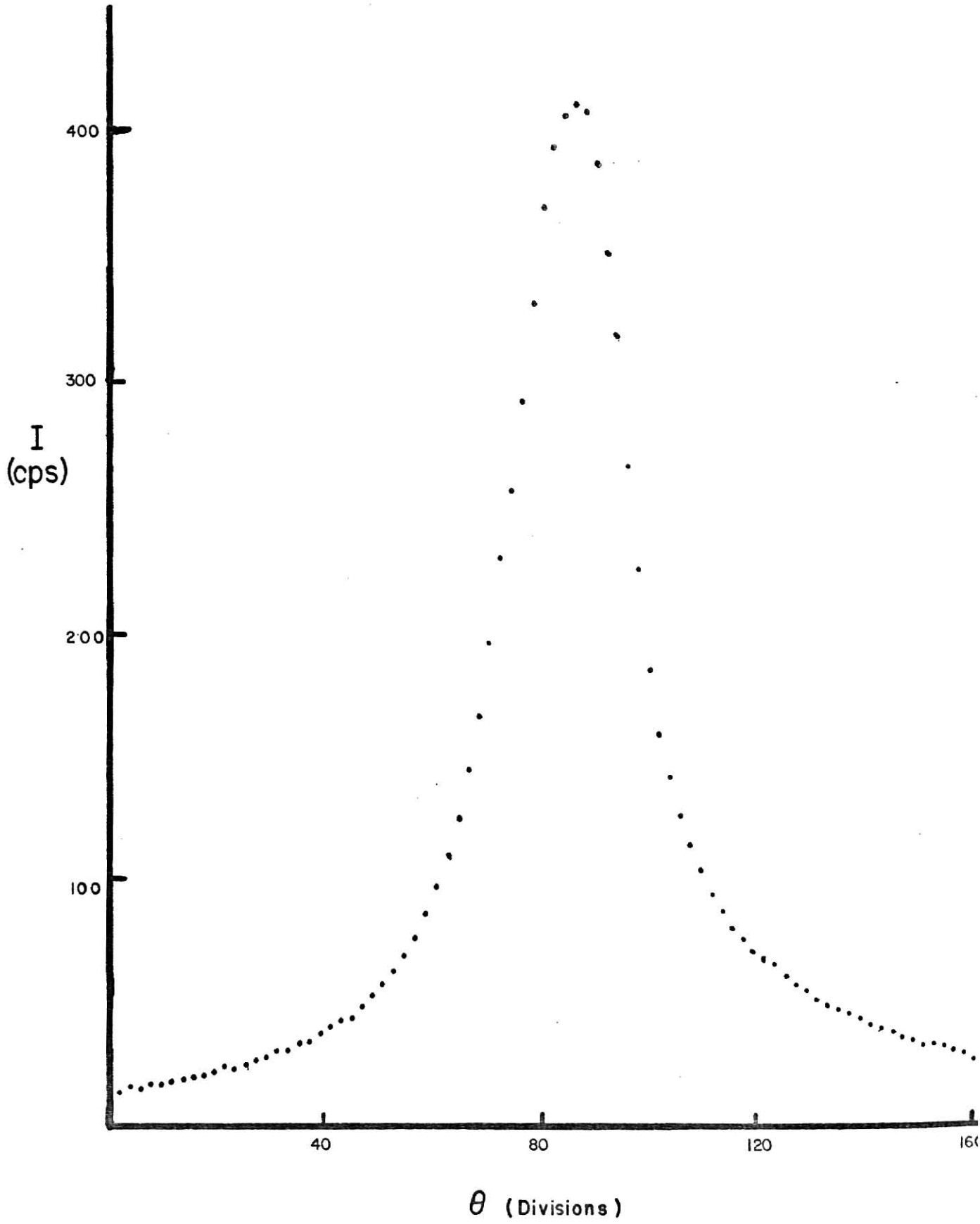

Figure 12. Rocking curve of unimplanted MgO. Although not typical, this curve is close to the 13.3 second FWHM predicted by the Darwin theory.

FIGURE 12

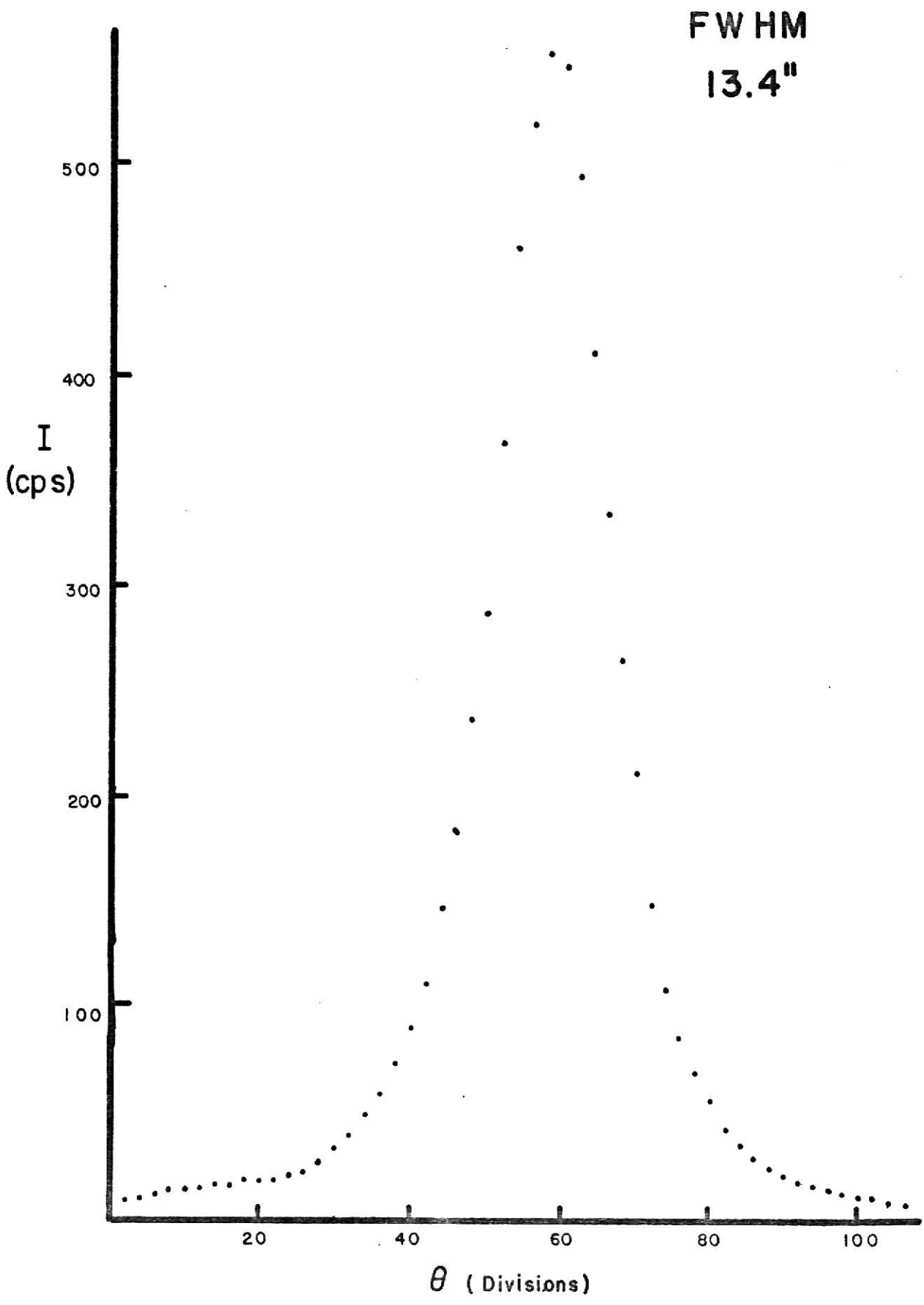

Figure 13. Four hundred division scan of both sides of a rocking curve of Rubidium implanted MgO. Note that no secondary peaks, as observed by Workman, are apparent.

FIGURE 13

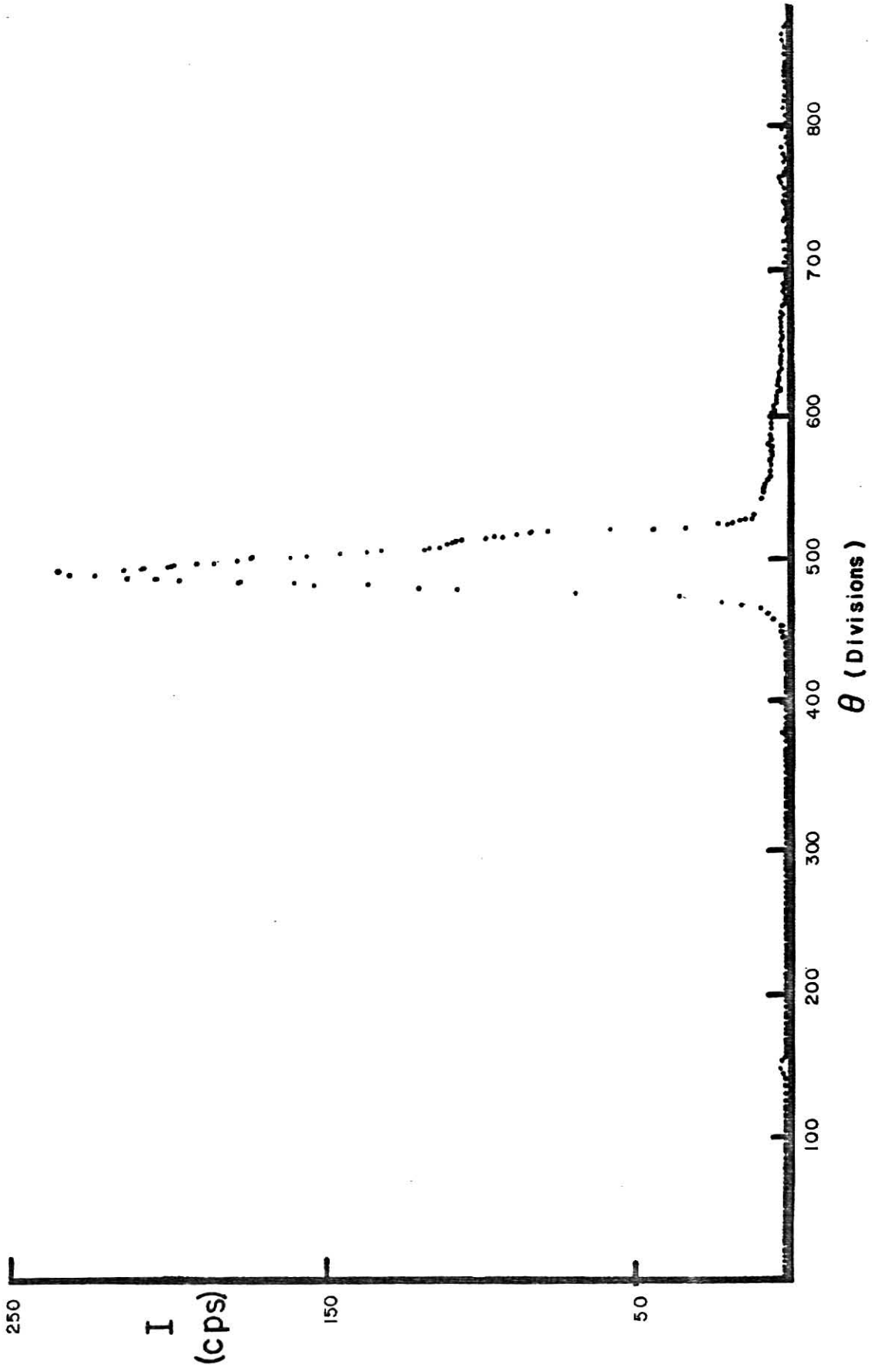

TABLE I

ROCKING CURVE FULL WIDTHS AT HALF MAXIMUM IN SECONDS OF ARC

Run I	Center of Crystal			Average	Mean Deviation	Edge of Crystal Left	Edge of Crystal Right
Argon	18.3	18.2	17.7	18.1	±0.2	26.6	33.8
Rubidium	17.7	18.8	18.4	18.3	±0.4	39.6	40.6
Unimplanted	16.2	17.8	17.6	17.2	±0.7	25.2	26.9
Run II							
Argon	20.1	20.7	21.4	20.8	±0.4	26.1	29.2
Rubidium	21.6	21.4	21.7	21.6	±0.1	32.9	28.6
Unimplanted	19.6	21.2	20.1	20.3	±0.6	31.8	28.2

Figure 14. Double crystal spectrometer angle calibration for the region of dial and wheel settings from $9944^{o}57'$ to $9945^{o}04'$ of turntable B. The angle conversion is 7.42 seconds = 10 divisions.

FIGURE 14

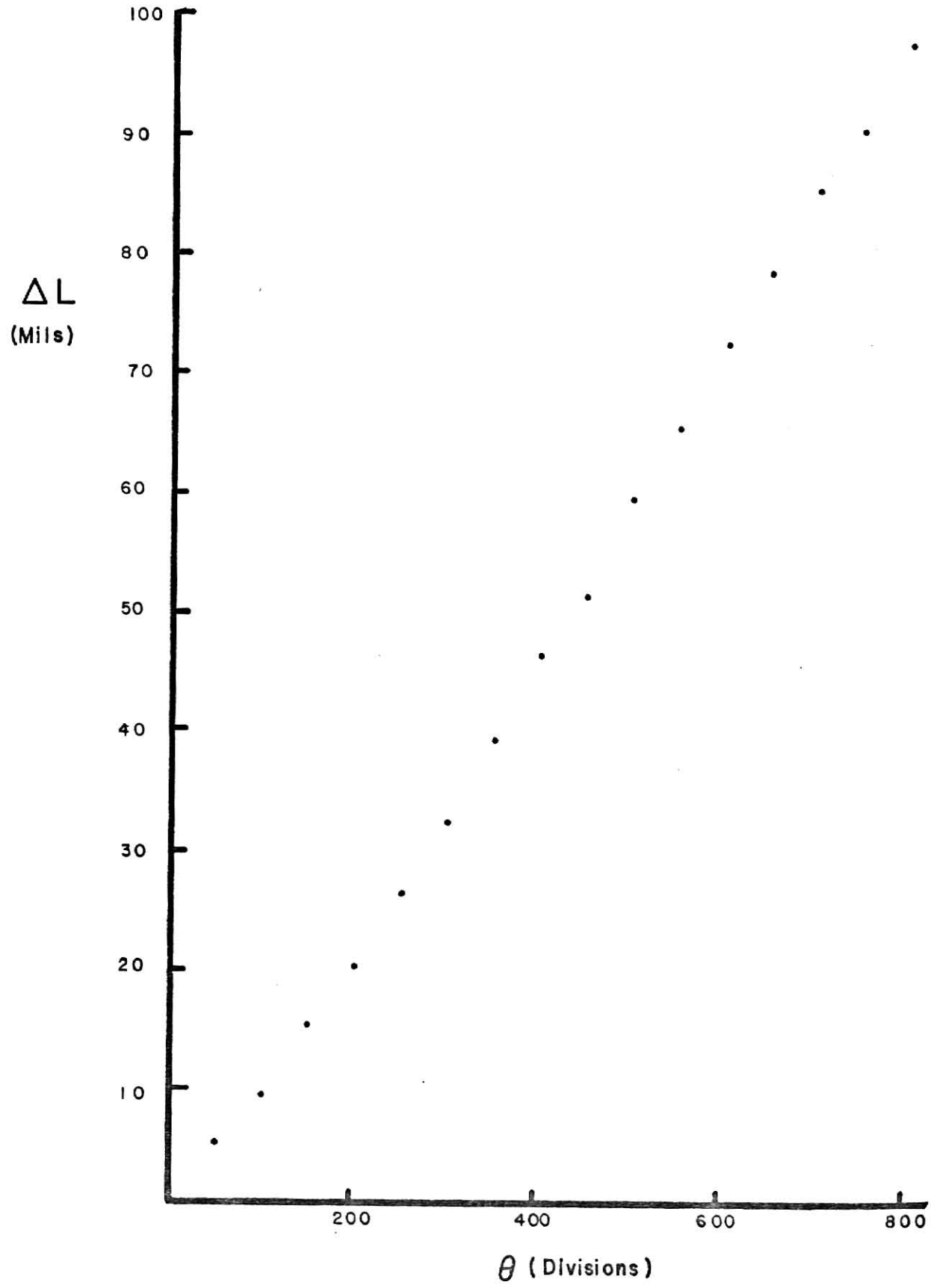

least squares fit to the data gave a slope of 0.0062 ± 0.0009 inches/10 divisions. This translates to a conversion factor of 7.4 ± 1 seconds/10 divisions.

DISCUSSION AND CONCLUSIONS

An examination of the results of Table I reveals a difference between Run I and Run II in the average rocking curve widths of both the implanted and unimplanted data. The average unimplanted width of Run II is about fifteen percent larger than Run I. The difference between the unimplanted curve and the Rubidium implanted curve is about six percent for both runs. The difference between the unimplanted curve and the Argon implanted curve is two percent for Run II and five percent for Run I. This may be due to switching the crystals to complete a run. The credibility of this idea is enhanced if one notes that the percent differences is the same in both runs for the Rubidium implanted and for the unimplanted crystal. This percent difference is not the same in the case of Argon. Recalling that the unimplanted widths were taken using the Argon crystal as the monochromator and that the Rubidium curves were taken without disturbing the first crystal, one can conclude that this discrepancy is due to an alignment problem in going from the Argon monochromator to the Rubidium monochromator. The problem may also be due to different single crystal widths of the different monochromating crystals.

Acknowledging this problem, we proceed to calculate the strain due to the implantation of ions using Eq. 26. Table II exhibits the results of these calculations.

TABLE II

CALCULATED STRAIN OF RUBIDIUM AND ARGON IMPLANTED CRYSTALS OF MgO

Run I	Center of Crystal	Edges of Crystal	
		Left	Right
Argon	$1.5 \pm 0.5 \times 10^{-4}$	$2.8 \pm 0.5 \times 10^{-4}$	$3.8 \pm 0.6 \times 10^{-4}$
Rubidium	$1.6 \pm 0.5 \times 10^{-4}$	$4.6 \pm 0.7 \times 10^{-4}$	$4.7 \pm 0.7 \times 10^{-4}$
Unimplanted	$1.4 \pm 0.6 \times 10^{-4}$	$2.7 \pm 0.5 \times 10^{-4}$	$2.9 \pm 0.5 \times 10^{-4}$
Run II			
Argon	$2.0 \pm 0.5 \times 10^{-4}$	$2.8 \pm 0.5 \times 10^{-4}$	$3.2 \pm 0.5 \times 10^{-4}$
Rubidium	$2.1 \pm 0.5 \times 10^{-4}$	$3.7 \pm 0.6 \times 10^{-4}$	$3.1 \pm 0.5 \times 10^{-4}$
Unimplanted	$1.9 \pm 0.5 \times 10^{-4}$	$3.6 \pm 0.6 \times 10^{-4}$	$3.1 \pm 0.5 \times 10^{-4}$

As a check on these results we wish to relate them to something which is familiar. The stress on a solid as a function of the strain in the solid and the Young's modulus of that solid is

$$F/A = Y_m \Delta d/d \qquad (27)$$

where Y_m is the Young's modulus of the solid, $\Delta d/d$ is the strain in the solid, and F/A is the force per unit area or the stress on the solid. The Young's modulus of magnesium oxide[23] is 2.45×10^{12} dynes/cm^2. The strain which we have computed is of the order of 10^{-4}. Substituting these numbers into Eq. 28, we obtain a stress of 2.45×10^{8} dynes/cm^2. The stress necessary to rupture an MgO crystal is some three orders of magnitude larger.

The FWHM of the Rubidium and Argon curves in both runs are larger than the unimplanted widths. As seen in the crossed polarizer photographs, the edges of both crystals are strained as is indicated by the funnel shaped light areas at the edges of the crystals. This strain is reflected in Table I as increased rocking curve widths. A variation of the strains inherent in the body of the crystal, as shown in the topographs, could easily account for the discrepancy in the rocking curve widths between Run I and Run II of Table I. A more careful experiment using a more nearly perfect monochromating crystal would decrease the uncertainty in the

difference of the actual measured widths.

A single rocking curve associated with the unimplanted lattice has been observed. Upon bombardment with ions of Argon and Rubidium, the symmetry of the rocking curve is unaffected. No secondary peaks were observed. The FWHM of the rocking curve was increased by an amount which yielded an order of magnitude result which is very reasonable for a simple model depicting the lattice as, on the average, strained in a manner in which one side of the lattice is compressed and the other side expanded about the implant concentration.

BIBLIOGRAPHY

1. R. Workman and R. D. Dragsdorf, B. Am. Phys. Society, 20, 377 (1975).
2. J. E. Thomas, T. O. Baldwin, P. H. Dederichs, Phys. Rev. B 3, 1167 (1971).
3. S. Kishino and A. Noda, Journal of the Japan Society of Applied Physics 42, 118 (1973).
4. B. Petry and M. Pluchery, C. R. Acad. Sci. Paris 272B, 240 (1962).
5. J. R. Patel, R. S. Wagner, S. Moss, Acta Metallurgica 10, 759 (1962).
6. K. J. Bachman, T. O. Baldwin, F. W. Young, Journal of Appl. Phys. 41, 4783 (1973).
7. C. G. Darwin, Phil. Mag. 27, 315 (1914); 27, 675 (1914).
8. P. P. Ewald, Ann. D. Physik 49, 1 (1916); 49, 117 (1916): 54, 519 (1917).
9. M. von Laue, Ergeb, der exact Naturwiss 10, 133 (1931).
10. R. W. James, The Optical Principles of the Diffraction of X-Rays, (G. Bell and Sons, Ltd., London, 1948), p. 52, 317.
11. W. H. Zachariasen, Theory of X-Ray Diffraction in Crystals, (J. Wiley and Sons, New York, 1935), Second Edition, p. 376.
12. A. H. Compton and S. K. Allison, X-Rays in Theory and Experiment, (D. Van Nostrand Co., New York, 1935), Second Edition, p. 376.

13. B. E. Warren, X-Ray Diffraction, (Addison-Wesly Pub. Co., Reading, Mass., 1969), p. 315.

14. L. V. Aza'roff et al., X-Ray Diffraction, (McGraw-Hill, New York, 1974), p. 222.

15. M. A. Krivoglaz and K. P. Ryaboshapka, Fiz. Metal. Metalloved. 15, 18 (1963).

16. J. Linhard, M. Scharff, H. E. Schiott, Mat. Fys. M. Dan. Vid. Selsk, 33 (1963).

17. J. Crawford and L. Slifkin, Point Defects in Solids, Plenum Press, New York, Volume 2, 1975), p. 71.

18. R. D. Dragsdorf, private communication.

19. J. Bearden, private communication.

20. S. Amelinckx, The Direct Observation of Dislocations, (Academic Press, New York and London, 1964), p. 44.

21. T. K. Ghash and F. J. P. Clarke, Brit. J. Appl. Phys. 12, 44 (1961).

22. R. Workman, An X-Ray Double Crystal Spectrometer Study of Singly-Ionized Sodium Implanted Magnesium Oxide, Master's Thesis, Kansas State University, 1974, p. 56.

23. C. Kittel, Introduction to Solid State Physics, (John Wiley and Sons, Inc., New York, 1971), p. 139, 150.

AN X-RAY DOUBLE CRYSTAL SPECTROMETER STUDY OF Ar and Rb IMPLANTED MgO CRYSTALS

by

BASIL LEE SNEERINGER

B.A., Kansas State College of Pittsburg, 197·

AN ABSTRACT OF A MASTER'S THESIS

submitted in partial fulfillment of the

requirements for the degree

MASTER OF SCIENCE

Department of Physics

KANSAS STATE UNIVERSITY
Manhattan, Kansas

1976

A technique using the double crystal x-ray spectrometer to study lattice damage has been demonstrated. A rocking curve of selected calcite was taken and an experimental FWHM was obtained and shown to be equivalent to the theoretical value for this crystal.

Angle calibration of the second crystal was made to allow measurements of 0.1 seconds of arc.

Qualitatively, strain was examined for the bulk crystals by the use of crossed polaroids and reflective x-ray topography.

A single symmetric rocking curve associated with two near perfect crystals of MgO has been observed. An average strain of 1.6×10^{-4} was obtained for the unimplanted crystals. Implantation of Ar and Rb ions showed a single rocking curve in which the symmetry of the unimplanted rocking curve has been preserved but with an increase in the FWHM. No secondary peaks were observed. The increase in the FWHM over the original FWHM of the unimplanted curves is attributed to the MgO lattice being strained to values of 2×10^{-4} with the uniform breadth of the symmetric curve indicating both compression and expansion of the original lattice in the vicinity of the implanted ions. Similar damage is introduced by the different ions at 60 keV.